RESEARCH PAPER

PCCP
www.rsc.org/pccp

The interaction of CO_2 with sodium-promoted W(011)†

F. Viñes,[a] A. Borodin,[b] O. Höfft,[b] V. Kempter*[b] and F. Illas*[a]

[a] *Departament de Química Física & Centre Especial de Recerca en Química Teórica, Universitat de Barcelona & Parc Científic de Barcelona, C/ Martí i Franquès 1, 08028 Barcelona, Spain*
[b] *Institut für Physik und Physikalische Technologien der TU Clausthal, 38678 Clausthal-Zellerfeld, Germany*

Received 21st June 2005, Accepted 30th August 2005
First published as an Advance Article on the web 15th September 2005

The activation of CO_2 by interaction with Na atoms on tungsten was studied in a joint experimental/theoretical effort combining MIES, UPS (HeII) and first principles calculations. Experimentally, both the adsorption of Na on tungsten, followed by CO_2 exposure to the Na-modified surface at 80 K, and the adsorption of CO_2 on tungsten, followed by Na exposure to the CO_2 covered substrate, were studied. Below about 120 K CO_2 physisorbs on pure W(011), and the distance between the three main spectral features is as for gas phase CO_2 (E_B = 8.4, 12.1, 14.1 eV). When offered to a Na monolayer (ML) deposited onto W, CO_2 is converted into a chemisorbed species. The spectral pattern is different from physisorbed CO_2, and the three spectral features are shifted towards lower binding energies (E_B = 6.3, 10.7, 13.9 eV). The chemisorption continues until all available Na species are converted into Na^+ species. Additional CO_2 offered to the system becomes physisorbed on top of the chemisorbed species. When a CO_2 monolayer, physisorbed on tungsten at 80 K, is exposed to Na, the interaction leads initially to a decrease of the surface work function and to a rigid, global shift of all CO_2 induced features towards larger binding energies by about 2 eV. Only beyond a minimum Na coverage of about 0.5 ML, chemisorbed species can be detected. We conclude that, initially, transfer of the Na(3s) electron to the tungsten substrate takes place. Above 0.5 ML Na coverage, back donation of charge to CO_2 takes place whereby the physisorbed carbon dioxide species become converted into chemisorbed ones. The experimental results are interpreted with the help of first principle calculations carried out on suitable slab models. The structures and surface binding mode of the chemisorbed CO_2 species are described. The calculated density of states for the most stable situations is in qualitative agreement with experimental data.

I. Introduction

The interest in CO_2 surface chemistry is considerable because of its relevance to several synthetic processes, for instance of urea, salicylic acid and methanol, and the need to reduce emission into the atmosphere. The carbon dioxide surface chemistry has been reviewed in the past,[1,2] and it is clear that the key step concerns its activation which usually requires charge transfer to CO_2, leading to a change in its bonding properties and electronic structure, and making $CO_2^{\delta-}$ more active than its predecessor. Essentially, one double bond has to be broken, resulting in a tilted form, with a three-center two-electron bond.

A widely used route to CO_2 activation is the co-deposition of donor species—alkali metals in particular—and CO_2 on metal surfaces. While CO_2 interaction with clean metal surfaces leads to physisorption, a strong chemisorption interaction occurs when these promoting species are present,[3] and may, *via* follow-up reactions, give rise to carbonate or oxalate formation, thus reducing the CO_2 amount in air and, at the same time, obtaining a useful product. Several experimental studies of co-deposition of CO_2 and alkali metals on the (011) surface of various substrates have been reported involving CO_2 adsorption on K/Cu,[4–8] Cs/Cu,[9] K/Fe,[6,10,11] Cs/Fe,[11] Na/TiO_2[12–14] and Cs/Ag.[15] Most of these previous works focus on methanol synthesis from activated CO_2, but the molecular aspects of CO_2 activations are not fully understood.

In the present work we explore the CO_2 + Na/W and Na + CO_2/W systems with the aim to disclose the molecular mechanisms of CO_2 activation on metal or on promoted metal surfaces. To this end, metastable impact electron spectroscopy (MIES) and ultraviolet photoelectron spectroscopy (UPS) are used. As compared to UPS, MIES possesses a rather large sensitivity for the detection of the Na(3s) electron, and its pronounced surface sensitivity allows, in combination with UPS, to distinguish between species adsorbed atop and underneath the surface under study. The corresponding spectra have been analyzed by state of the art first principles methods. For the CO_2 + Na/W(011) system, no previous experimental or theoretical studies are available in the literature although the present study is closely related to previous ones concerning CO_2 adsorption on K promoted Fe surfaces.[6,10,11] This is because of the similar crystal structure of W and Fe; both following a body centered cubic packing (bcc) and, also, the close similarity between the chemical behavior of Na and K.

This paper is organized as follows: section II reports the experimental setup and describes the most important experimental data; section III outlines some computational details; section IV describes the interaction of CO_2 on W(011) while section V reports the results corresponding to the interaction of Na on W(011) and for the co-adsorption deposition of CO_2 and Na in W(011). Finally, section VI summarizes the main conclusions of the present work.

II. Experimental remarks

The experiments, described in detail elsewhere,[16,17] were carried out under ultra high vacuum (UHV) conditions (base pressure $<2 \times 10^{-10}$ Torr). AES and XPS are used to characterize the chemical composition of the tungsten substrate employed for the deposition of the molecular films. The

† Colour versions of Figs. 1, 5, 6, 7 and 8. See http://dx.doi.org/10.1039/b508748a

DOI: 10.1039/b508748a

electronic structure of the molecular films was studied by applying MIES and UPS. In MIES, metastable helium atoms eject electrons from the edge of the surface under study. The application of MIES to surface spectroscopy is well documented.[18,19] When the Na adsorbate is not fully ionized, a spectral feature, denoted as Na(3s), is expected from the presence of 3s charge density at the Na core; it occurs near to the Fermi level and is clearly seen on metals and semiconductors for coverages larger than about 0.5 ML.[18,19] At this and higher coverages Auger de-excitation (AD) and auto-detachment of He^{-}* species formed by electron attachment to the metastable He* probe atoms both contribute to Na(3s). Thus, other than for AD process, the shape of the feature does normally not image the partial DOS of Na.[18,19] With UPS (HeI and II), a partially occupied Na(3s) level is practically not seen due to small photoionization cross sections.[20] This underlines the power of MIES for investigating the chemistry between Na and molecular films, which can be expected to be driven by the 3s valence electron. In the present work, dedicated to the study of the Na-induced changes in the electronic structure of CO_2 and Na films, we have confined ourselves to reporting MIES and UPS(HeII) spectra.

The experiment produces energy spectra of the emitted electrons *versus* their kinetic energy. By choosing a suitable bias voltage between the target and the electron energy analyzer, the energy scales in the figures are adjusted in such a way that electrons emitted from the Fermi level, denoted by E_F, *i.e.* electrons with the maximal kinetic energy, appear at 19.8 eV (which is the potential energy of the metastable He atoms employed for MIES). The position of E_F is determined from MIES spectra for Na-covered tungsten. With this particular choice of the bias voltage, the low-energy cutoff in the spectra gives directly the surface work function (WF), irrespective of the actual interaction process which produces the electrons. In order to allow a convenient comparison with theory we present our data as a function of the binding energy of the emitted electrons prior to their ejection. Electrons emitted from the Fermi level, *i.e.* those with the 19.8 eV kinetic energy, appear at binding energy $E_B = 0$ eV with respect to the Fermi level.

Na atoms were dosed employing carefully outgassed commercial dispenser sources (SAES Getters), operated at a rate of 0.05 ML min^{-1}, typically. The procedure for the calibration of the alkali coverage is described elsewhere.[21] The Na exposure is given in units of monolayer equivalents (MLE); at 1 MLE the surface is covered by one Na monolayer as long as penetration of the Na into the CO_2 film can be neglected. The surface temperature can be varied between about 80 and 600 K; the accuracy of the temperature calibration is 10 K. The surface was exposed to CO_2 by backfilling the chamber. Prior to Na exposure the surface prepared as described above was cooled to the desired temperature. The calibration of the Na film thickness was made in the following manner. It is assumed that the WF minimum occurs at 0.6 ML (this has been indeed confirmed by the present theoretical calculations), and that the sticking coefficient, at 80 K, is constant throughout the entire exposure range, *i.e.* also at exposures that lead to coverages larger than 1 ML.

For CO_2, we obtain an estimate for the coverage at 80 K by comparing the MIES and HeII spectra. On the one hand, MIES shows very little substrate emission and, on the other hand, with HeII the substrate emission is little attenuated by the offered CO_2; furthermore, the CO_2-induced signal does not change anymore above 5 L. Thus, from MIES we conclude that we have produced a closed CO_2 layer while HeII indicates that the coverage produced at 80 K cannot be more than one complete layer.

III. Computational details

The calculations were carried out in the framework of the density functional theory (DFT) within the generalized gradient approximation (GGA), using the implementation proposed by Perdew *et al.*[22] for the exchange–correlation functional; hereafter this is referred to as PW91. A plane-wave basis set was used to expand the valence electronic states and the core electrons were represented by the projected augmented wave (PAW) method of Blöchl.[23] This permits to obtain results which are similar to those obtained using all electron frozen core methods but within the computational simplicity of the pseudopotential approach, especially in the implementation of Kresse and Joubert.[24] This representation of the core states allows one to obtain converged results with a cut-off kinetic energy of 415 eV for the plane-wave basis set. A Monkhorst–Pack grid has been used to select the special *k*-points necessary to carry out numerical integrations in the reciprocal space. The number of *k*-points in each direction has been adapted until total energies computed with increasing sets of *k*-points differ by less than 0.01 eV. The grid for W is 15 *k*-points/direction, and 13 *k*-points/direction for Na. The cutoff kinetic energy was also optimized, setting it to 230 eV for metallic W, 300 eV for Na adsorbed on W and also in metallic sodium, and to 415 when the surfaces interact with carbon dioxide. The latter cutoff value has always been used to compute adsorption energies of CO_2 on the different surfaces. The structural optimization was performed using a conjugated gradient technique in which the iterative relaxation of atomic positions was stopped when the change in the total energy between successive steps was less than 0.001 eV. With this criterion, forces on the atoms are generally smaller than 0.1 eV $Å^{-1}$. A comparison between calculated and experimental values indicates that the error on the calculated cell parameter for both Na and W is less than 1%.

Once the optimum lattice parameter was determined for each metal, a slab model for W(011) surface has been constructed, this is because experiments have been carried out for this particular surface which indeed is the most stable one for a bcc crystal. In this approach one uses a unit cell which is repeated periodically in two dimensions while it has a finite extent in the third one. In order to use the plane wave basis set, which is periodic in nature, the corresponding slab is repeated in the third direction with the slabs separated by a sufficiently wide vacuum region. A vacuum width of 10 Å has proven to be large enough for the present purposes. The W(011) slab models contain three atomic layers and the two outermost atomic layers were fully relaxed in these and subsequent calculations using the optimization procedure outlined above. Test calculations using an increased number of layers show that, for the present purposes, results can be considered as converged with respect to slab thickness. For the slab model, the *k*-point grid in the 011 direction has been reduced to 1. A rather small inward relaxation of $\sim$3% has been found in agreement with the experimental trend found for most metal surfaces.

All electronic structure calculations were carried out with a parallel version of the VASP 4.5 code[25–27] implemented in an IBM SP4 machine and on Linux clusters.

IV. CO_2 adsorption on W(011)

In order to model the interaction of CO_2 with W(011), CO_2 molecules have been placed above the surface in two probable adsorption sites. These correspond to alignment of the O–C–O axis with either the long bridge or the short bridge, with C directly on top of a W atom and the molecular axis parallel to the surface. Nevertheless, the position of the oxygen and carbon atoms was independently optimized. In all cases the energy optimization process results in weakly adsorbed molecules with geometries nearly identical to that of the gas phase with a linear structure and distances of 1.16 Å. The very small adsorption energies which indeed are positive already indicate that the interaction is very weak, as expected for a

physisorption process. In principle, one would expect a small but negative value, the fact that the calculated value is positive is a consequence of the limitation of the current GGA functionals which are well-known to have difficulties in correctly describing weak interactions.[28,29] However, even if the final geometries and adsorption energies are not really accurate, there is clear indication that the interaction is very weak, and the molecular structure is that of the gas phase. A graphical representation of the 3-D projection of the charge density—not shown—evidences that the electronic densities of the CO_2 molecule and of the tungsten surface remain unperturbed. The conclusion about the weak interaction of CO_2 with the tungsten surface is reinforced by the analysis of the local projected density of states (LDOS) reported in Fig. 1 which shows no evidence of charge-transfer from the metal to CO_2. Moreover, it shows clearly that the CO_2 -related one electron levels (*i.e.* orbital energies) remain unaltered, except for a slight broadening of the $1\pi_u$ level due to its different interaction with the surface. In fact, one of the $1\pi_u$ orbitals is slightly stabilized due to proper interaction with tungsten d-orbitals, but not enough to distinguish between them. As a result, a broadening is observed only. A similar argument explains the broadening of the $1\pi_g$ level resulting in a more-stabilized and broader level because of a more favorable interaction with the surface and in an essentially unaltered orbital.

Both MIES and UPS(HeII) display the structure denoted by CO_2(phys) (Figs. 2 and 3, top spectra), observed after CO_2 deposition onto neat W(011) at $T < 120$ K. For deposition at 80 K, CO_2(phys) starts to decrease around 100 K (see Fig. 4), typical for a physisorbed species; the most weakly bound species probably corresponding to those adsorbed on terraces, as modeled by the present DFT calculations. In MIES, CO_2 (phys) consists of broad peaks at $E_B = 8.1$; 12.0 eV (labeled $1\pi_u$ and $1\pi_u$; $3\sigma_g$, respectively); an indication of an additional feature ($4\sigma_g$) is seen with HeII at $E_B = 13.5$ eV. From the analysis of energy levels differences listed in Table 1, one can readily see that the calculated values match those obtained from the MIES and UPS spectra for the same system which show energy differences of 3.9 eV between the double degenerated $1\pi_g$ orbitals and the broad feature corresponding to the $1\pi_u$ and $3\sigma_u$ orbitals—which because of the weak interaction with the surface appear as a single broader peak—and of 1.5 eV between the last one and the $4\sigma_g$ orbital. The calculated values from the density of states are 3.5 and $\sim$1.1 eV, respectively, which are close to the experimental ones. The constant difference of 0.4 eV in the energy levels difference with respect to the experiment is probably due to the inherent limitations of the PW91 method to properly describe this weak interaction.

Provided that the HeII spectra represent the DOS of the occupied states, *i.e.* no final state effects important, the total tungsten DOS (see Fig. 1) can be compared with the intensity in the HeII spectra for pure tungsten (see Fig. 3, bottom). Indeed, general agreement is found as far as the positions of the major structures, in particular the minima in DOS and UPS (HeII) spectra around 4 eV are concerned.

To sum up, CO_2 on W(011) remains almost unaltered as compared to the gas phase, with no evidence for charge transfer from the substrate to the molecule and, hence, no evidence of activation, in complete agreement with experimental findings.

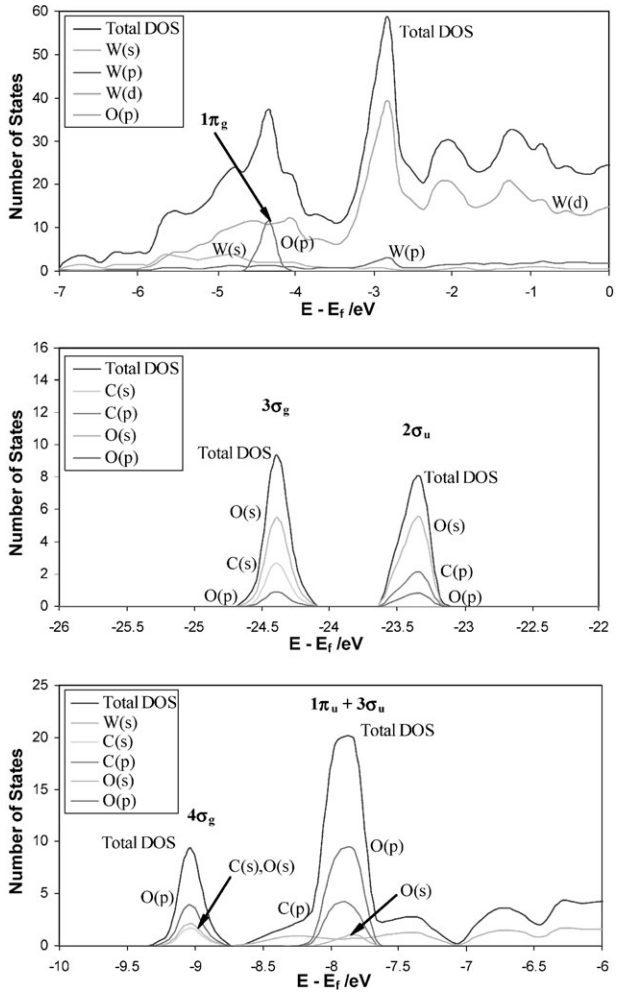

Fig. 1 Local projected density of states (LDOS) of CO_2 adsorbed on W(011). Total DOS, and projections on both atoms and related orbitals are shown—W(d) is the density of states associated to the 5d orbitals of tungsten, C(p) to the 2p orbitals of carbon, *etc.*

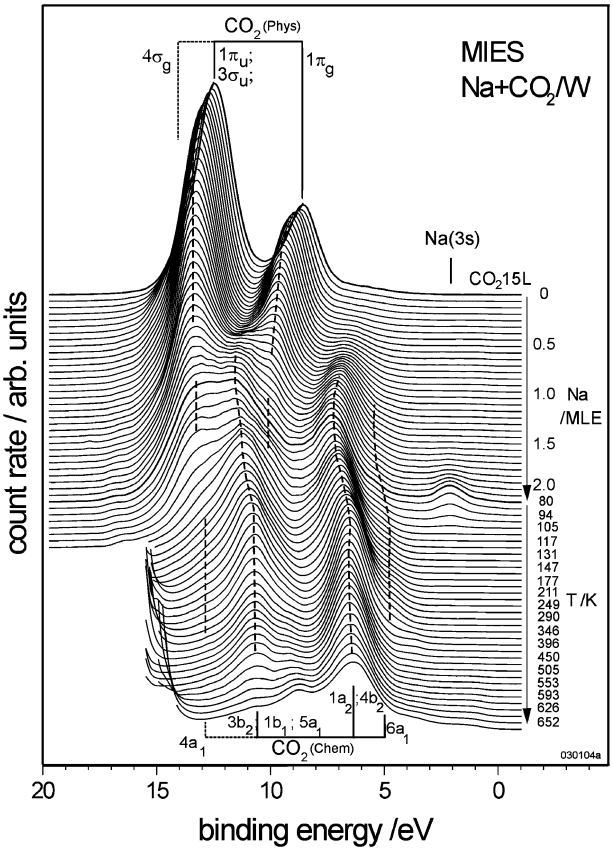

Fig. 2 MIES spectra for interaction of Na with a CO_2 monolayer prepared on tungsten (80 K) as a function of Na exposure (upper set of spectra), and the spectral changes resulting when annealing the Na/CO_2 system over the indicated temperature range (lower set of spectra) (see text for the acronyms employed in the figure).

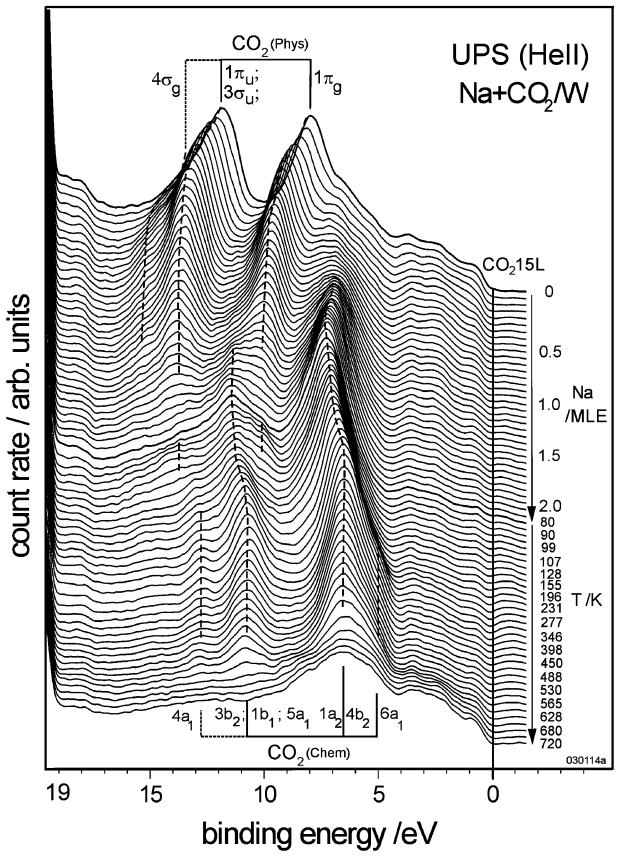

Fig. 3 UPS(HeII) spectra for the interaction of Na with a CO_2 monolayer prepared on tungsten as a function of Na exposure (80 K) (upper set of spectra), and the spectral changes resulting when annealing the Na/CO_2 system over the indicated temperature range (lower set of spectra).

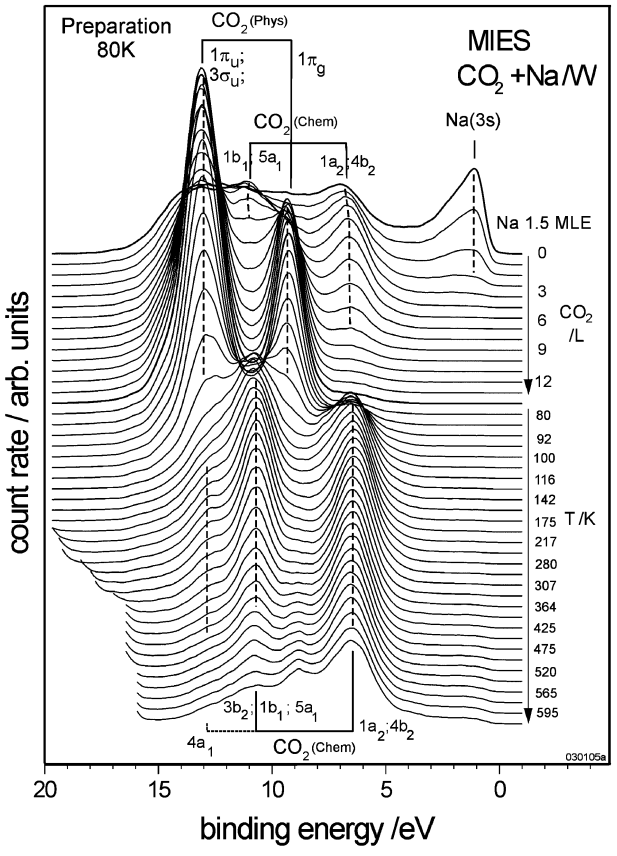

Fig. 4 MIES spectra for the interaction of CO_2 on Na (1.5 layers) prepared on tungsten held at 80 K (upper set of spectra), and the spectral changes resulting from film annealing the CO_2/Na system over the indicated temperature range (lower set of spectra) (see text for the acronyms employed in the figure).

V. Na adsorption and CO_2/Na interaction on W(011)

V.1. Na adsorption on W(011)

Several models have been built in order to find the most favorable sites for Na adsorption on W(011) surface. Those involve ontop, bridge and four-fold hollow high symmetry adsorption sites. The adsorption of sodium on each site has been evaluated at three different coverages (θ) of 1/8, 1/4 and 1/2. Na atoms have been placed at an initial distance of 2.5 Å above the surface and next Na have been allowed to relax along the [011] direction. Adsorption energies, E_{ads}, have been calculated as the difference of the adsorbed system and the sum of the clean surface and spin polarized isolated sodium atom in a cubic box of 10 Å. In this case a 415 eV energy cut-off has been used.

From the adsorption energies reported in Table 2, one can see that the differences between different high symmetry sites are rather small. Moreover, in all cases, when increasing the Na coverage, the adsorption energy decreases in the range 0.125 to 0.5 ML due to the repulsion between the positively charged alkali adsorbates. At even higher Na coverage, metallic bonding develops between the adsorbed Na atoms with a concomitant decrease of ionicity of the Na–W interaction. In order to model the experimental conditions employed in Fig. 4, from all sites and coverage values for Na adsorbed W(011) considered in the present work, the one representing the most stable site at the highest possible coverage has been chosen. This corresponds to the four-fold site with $\theta = 1/2$ and to a 4×4 supercell. In this supercell the Na atoms are separated by 7.81, 6.38 and 4.51 Å, respectively, as shown in Fig. 5.

The MIES results for Na on W(011) (Figs. 4 and 6, top) do not allow for a direct comparison with the results predicted from theory: as mentioned above, the strong Na(3s) feature at

Table 1 Geometry of the CO_2 molecules adsorbed on W(011), d(CO), $d_\perp$ and α(OCO) correspond to the C–O distance, the vertical distance from the C atom to the surface and the O–C–O internal angle, respectively. Distances are given in Å and angles in degrees. E_{ads} stands for the calculated adsorption energy. Positive values of E_{ads} indicate a bound system and *vice versa*. The energy difference between CO_2 related peaks in the density of states is also given. All energies are in eV. For comparison, the rightmost column reports the data for free CO_2 as obtained using the same computational setup

	Short	Long	Free CO_2
d(CO)	1.18	1.18	1.18
α(OCO)	180.0	179.8	180.0
$d_\perp$	3.41	3.40	
E_{ads}	0.07	0.06	
$2\sigma_u - 3\sigma_g$	0.91	1.06	1.01
$4\sigma_g - 2\sigma_u$	14.43	14.28	14.37
$(1\pi_u + 3\sigma_u) - 4\sigma_g$	1.06	1.22	1.15
$1\pi_g - (1\pi_u + 3\sigma_u)$	3.49	3.50	3.52

Table 2 Adsorption energies (in eV) of Na atoms on top, bridge and hollow sites at 1/8, 1/4 and 1/2 coverages

θ	1/8	1/4	1/2
Top	−2.25	−2.14	−2.03
Bridge	−2.31	−2.20	−2.10
Four-fold	−2.36	−2.25	−2.15

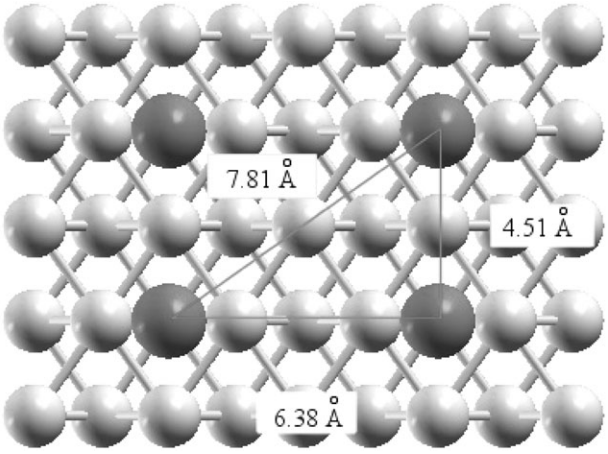

Fig. 5 Distances between adsorbed Na atoms in the 4 × 4 supercell.

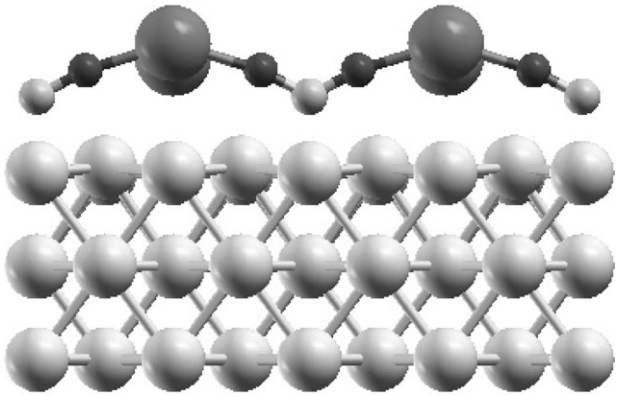

Fig. 6 Final structures of the long–long conformation (see Table 4) of the adsorption of carbon dioxide on Na-decorated W(011).

E_F, being mostly due to auto detachment of He^-*$(1s2s^2)$ species,[18] does not provide a direct image of the Na partial DOS. From the projected DOS of Na derived levels near E_F it is however possible to argue that there is a net charge transfer from Na to W; this is further discussed in the next section.

V.2 CO_2/Na interaction on W(011)

Fig. 4 reports MIES spectra of CO_2 interacting with a 1.5 ML thick film of Na on tungsten. Impinging CO_2 becomes activated, and the species CO_2(chem) characterized by peaks at $E_B = 6.4$; 10.8 eV (labeled $1a_2$;$4b_2$ and $3b_2$;$1b_1$;$5a_1$, respectively) is produced exclusively (<3 L). As compared to CO_2(phys), the peaks are shifted towards lower binding energies by about 1.7 eV, and their distance is larger by about 0.5 eV. Moreover, the two species, CO_2(phys) and CO_2(chem), display a rather different dependence on the substrate temperature: while CO_2(phys) has desorbed around 120 K, CO_2(chem) is rather stable, and not before 400 K does its signature disappear from the spectra. Chemisorption continues only as long as 3s charge density is present at the Na^+ cores, *i.e.* it stops when Na(3s) has disappeared. Additional CO_2 leads then to physisorption on top of the Na-modified layer. This follows from the correlation seen between the growth of the structure CO_2(phys) at the expense of CO_2(chem) which finally disappears for >10 L. The physisorbed layer desorbs around 115 K whereby CO_2(chem) reappears (now displaying an additional third peak at E_B = 13.8 eV), remaining visible up to $T > 500$ K. If the CO_2 layer is produced at 120 K (not presented), the initial stage of the interaction is as at 80 K, but no physisorption takes place on top of the chemisorbed layer. In principle, CO_2(chem) could be due to carbonate (CO_3) formation. In fact, the CO_2 interaction with alkaline earth (M) films (M = Mg, Ca, Sr, Ba) leads to CO_3 formation. It was suggested that in the early stage of exposure CO_2 becomes dissociated, and (M–O) bonds are formed.[30–33] Further exposure leads to CO_2 chemisorption at these surface-adsorbed oxygen atoms, thereby forming CO_3 complexes. In the present case, no indication for the formation of (Na–O) bonds is seen, and the spectra do not resemble closely those from CO_3 species. Thus, we tend to exclude CO_3 species as the origin of CO_2(chem).

The experimental situation studied in Figs. 2 and 3 provides additional insight into the conditions under which CO_2(chem) is formed: the tungsten substrate, pre-covered by 1 ML CO_2 at 80 K, displays only CO_2(phys), *i.e.* a physisorbed film has been produced. Exposure to Na leads to a decrease of the work function by about 2 eV. In the early stage we notice the complete absence of Na(3s) feature which would signal the presence of the 3s electron at the Na^+ core. The decrease of the work function shows however that Na^+ species become adsorbed even at the earliest exposure stage. We conclude that the Na(3s) electron is transferred to the CO_2/W interface. On the other hand, up to 0.5 MLE no chemisorbed species is formed as a consequence of the transfer of the Na(3s) electron, neither in MIES nor UPS. The structure CO_2(phys) merely shifts simultaneously with the work function whereby the energetic distances between the spectral features remain conserved.

CO_2 chemisorption does, however, occur for exposures larger than 0.5 MLE, as manifested by the appearance of CO_2(chem), correlated with a decrease of the CO_2(phys) intensity. Thus, we are led to the conclusion that a minimum Na supply, equivalent to about 0.5 ML coverage, is required to start CO_2^- formation. The co-deposition of alkali atoms and CO_2 on titania at room temperature leads to similar threshold behavior, in this case for the CO_3 formation.[34–36] Above about 1.7 MLE Na atoms become adsorbed as neutral species as manifested (see Fig. 2) by the appearance of the peak Na(3s), about 2 eV below the Fermi level.

In Figs. 2 and 3 a shoulder can be noticed at the low-binding energy side of the ($1a_2$; $4b_2$) peak. We attribute this shoulder to an additional spectral feature located at about $E_B = 4.5$ eV. This is an indication that charge transfer takes place from the Na–W system to the CO_2 adsorbates, leading to the partial population of previously unoccupied MOs during the chemisorption process (see below).

When modeling the CO_2–Na interaction, there are several possibilities of adding a CO_2 molecule to the Na–W supercell. Placing CO_2 in the middle of the diagonal corresponding to a Na–Na distance of 7.81 Å (*cf.* Fig. 5) has been rejected because, at full coverage, this site would be occupied by a Na atom and because the interaction with neighboring Na results either in a too long Na–O distance or in an unfavorable orientation. Adsorption in the middle Na–Na atoms separated by 6.38 Å, hereafter referred to as long–long, has been checked, but only along the Na–Na direction. The perpendicular orientation would imply a too long Na–O distance. Therefore, for the interaction of CO_2 along the 4.51 Å Na–Na distance situation, the only possible way to compare to the situation corresponding to CO_2 interaction with the clean W(011) surface, described in the previous section, implies placing the CO_2 molecule in the middle of the Na–Na atoms separated by 4.51 Å. In this case one can still place the CO_2 molecule following the Na–Na direction (long and long-top orientations) or perpendicular to it (cross). In these spacial dispositions, the unit cell is reduced to a 4 × 2 supercell. Starting from these geometries the molecular structure of the CO_2 molecule has been allowed to fully relax with no constraints. The final optimized structures are reported in Table 3 and the long–long configuration is depicted in Fig. 6.

The first important result is that the interaction along the long direction is largely unstable. It results in a highly stressed

Table 3 Structural parameters for the final optimized geometries of CO_2 on the Na decorated W(011) surface. This corresponds to the cross, long and long-top conformations for the 4.51 Å direction (cases A, B and C, respectively, see Fig. 7), and long–long for the 6.38 Å direction (case D), all described in Fig. 5. d(CO) and d(OO) are the interatomic distance whereas d(s–C) and d(s–Na) are the perpendicular distances of C and Na to the surface, respectively. Distances (d) are given in Å, angles (α) are given in degrees. E_{ads} are given in eV molecule^{-1} and calculated from the Na/W(011) system

	Cross	Long	Long-top	Long–long
d(CO)	1.20	1.49	1.17	1.29
d(s–Na)	2.62	2.49	2.66	3.04
d(s–C)	3.61	2,02	4.78	1.78
α(OCO)	160.14	58.32	179.48	123.15
d(OO)	2.36	1.47	2.34	2.27
E_{ads}	0.58	5.23	−0.24	−1.34

structure with a very high energy. From the three remaining structures, the one termed long-top involves an almost linear CO_2 molecule. The analysis of the DOS shows that this is very similar to the configuration corresponding to the interaction of CO_2 with the clean W(011) surface. The CO_2 energy level pattern is the same as in the adsorption on clean tungsten (see Fig. 1), with a very small split in the $1\pi_u$ and $3\sigma_u$ levels and with the entire pattern shifted towards higher binding energies by about 2.7 eV. The main interactions are with Na, but are still sufficiently small for CO_2 to maintain its gas phase structure. Hence, the long-top interaction leads to a physisorbed species which is only slightly more stable than the one corresponding to the clean metallic surface because of some electrostatic interaction with the adsorbed Na atoms. The two remaining optimized structures, above defined as cross and long–long, present a highly distorted CO_2 molecule with a OCO angle which for the cross conformation is now 160° and, hence, reminiscent of CO_2^-. The cross structure is slightly unstable with respect to the Na-covered W(011) surface plus gas phase CO_2 but it is, of course, stable with respect to separated CO_2, Na and the W(011) surface. In any case, the vibrational analysis confirms that this structure is a minimum on the potential energy surface, because all normal vibrational modes of carbon dioxide present real frequencies. The analysis of the projected density of states of this structure already indicates charge transfer from the Na s-orbitals to the W conduction band thus providing extra electron density which, therefore, can be donated to the CO_2 molecule. This is confirmed by the projected density of states for Na adsorption on the clean W(011) surface, where the extremely low projected DOS of Na derived levels in the energy range around the Fermi level suggests a net charge transfer from Na to W. This is indeed the typical situation for alkali atoms adsorbed on metal surfaces,[37] also seen here for Na coverages up to about 0.3 MLE.

The long–long conformation is the most revealing one; the corresponding structure is very close to that of gas phase CO_2^- with the OCO angle being 123° close enough to the 135 for CO_2^-.[2] The electron transfer from the substrate to the CO_2 molecule is facilitated by the work function decrease. In fact, the calculated value for the W(011) is 4.88 eV, in good agreement with the experimental value of 5.05 eV.[38] The calculated value for a coverage of 0.5 ML is 1.81 eV implying a decrease of almost 3 eV. This is in very good agreement with the observed experimental decrease at 0.6 ML which is of 2.9 eV. Notice that this is similar to the structure found for CO_2 on a K covered Pt(111) surface.[3] However, the model used to represent the Pt(111) surface was more limited and a direct comparison is difficult. Still, the close resemblance in the structure of the adsorbed molecule and the conclusion that a direct interaction between CO_2 and the K is necessary to stabilize the former are in agreement with present findings. The mere electron transfer donation from the alkali metal to the substrate is not enough and further stabilization is provided by the electrostatic interaction between the alkali cation and the negatively charged CO_2 molecule. Notice also that in the work of Ricart *et al.*[3] the structures, equivalent to the present long–long and cross conformations, were found to be almost degenerate in energy. Here, the long–long structure is clearly the most stable one. This is because it maximizes the interaction between the two charged adsorbed species. Notice that the Na–O distance is comparable to that in the Na carbonate structure. In this conformation, the interaction of CO_2 on the Na covered W(011) surface is accompanied by a weak relaxation of the neighboring Na atoms which relax outwards by ~0.4 Å. The final perpendicular distance from Na to the W surface is 3.04 Å, considerably longer than the values corresponding to the other conformations (Table 3). This can be viewed as a way to better accommodate the charged carbon dioxide molecules.

Returning to the cross conformation, the splitting of the $1\pi_u$ and the $3\sigma_u$ orbitals, as well as of the $1\pi_g$ levels is concomitant with the structural change of the adsorbed molecule. Now, Table 4 reports the differences between consecutive energy levels for both the cross and long-top cases. For the cross case, the $1a_2 - (1b_1 + 5a_1)$ and $3b_2 - 4a_1$ energy differences are too small to match the experimental result. The experimental splittings are 4.4 and 2.1 eV, respectively, whereas the values derived from the calculated DOS are of 3.6 and 1.1 eV. The splitting of the $1\pi_u$, $3\sigma_u$ and $1\pi_g$ levels is also seen in the LDOS of the long–long conformation (Fig. 7), but also a larger charge transfer and the splitting of $1\pi_u$ and the $3\sigma_u$ orbitals which now results in three clear peaks. Notice that for the $1\pi_g$ levels a broadening of this level appears. The energy differences between these peaks are now (long–long case) 3.2 and 1.98 eV for the $1a_2 - (1b_1 + 5a_1)$ and $(3b_2 - 4a_1)$ separations, respectively. The last one is now closer to the experimental value of 2.1 eV.

The inspection of the Walsh diagram of the CO_2 molecular orbitals and the Mullikan population on cluster models suggest that for a bonding angle of 123° emission from the partially occupied anti-bonding $\pi^*(6a_1)$ can be expected near the position of the structure $(1a_2;4b_2)$. Indeed, the structure denoted by $6a_1$ in Figs. 2 and 3 can be attributed to the ionization of the

Table 4 CO_2 molecular orbital energy differences (in eV) in all the adsorption possible conformations on the Na decorated W(011) surface

Long-top		Cross		Long–long
$2\sigma_u - 3\sigma_g$	0.93	$2b_2 - 3a_1$	1.17	$2b_2 - 3a_1$	1.98
$4\sigma_g - 2\sigma_u$	14.31	$4a_1 - 2b_2$	14.00	$4a_1 - 2b_2$	10.95
$(1\pi_u + 3\sigma_u) - 4\sigma_g$	1.17	$3b_2 - 4a_1$	0.93	$3b_2 - 4a_1$	1.98
$1\pi_g - (1\pi_u + 3\sigma_u)$	3.62	$(1b_1 + 5a_1) - 3b_2$	0.35	$(1b_1 + 5a_1) - 3b_2$	0.61
		$1a_2 - (1b_1 + 5a_1)$	3.38	$1a_2 - (1b_1 + 5a_1)$	3.20
		$4b_2 - 1a_2$	0.23	$4b_2 - 1a_2$	NA

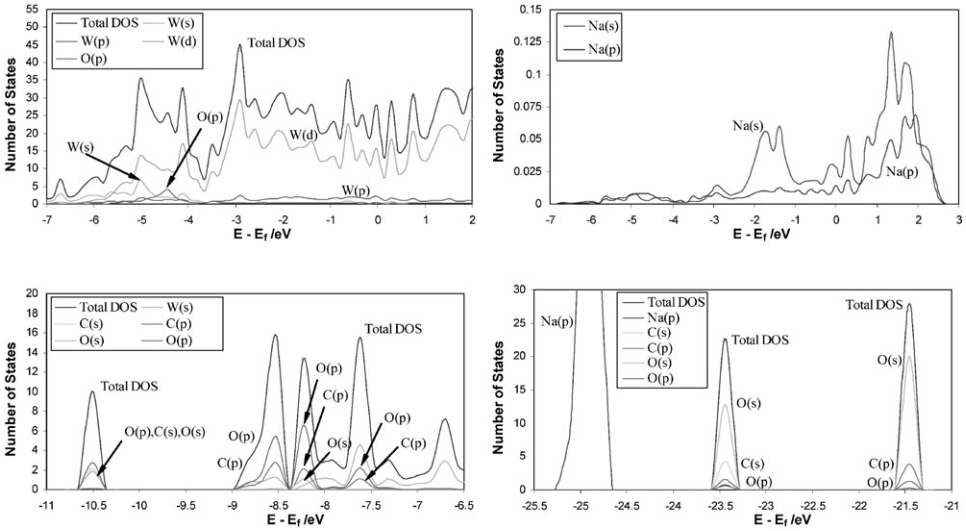

Fig. 7 LDOS of CO_2 (long–long conformation).

partially occupied π*-type $6a_1$ MO. In addition, one can also speculate that the structure seen in the Na LDOS (Fig. 7) between 1 and 2 eV gives rise to a peak appearing around 2 eV in the MIES spectra when Na becomes adsorbed as neutral species.

The charge transfer to CO_2 found for the cross and long–long structures merits some additional comment. In fact, one may wonder whether the charge transfer is directly from the Na atoms or is mediated by the surface. To answer this question, Fig. 8 reports the projected DOS for the two structures described above and for the long-top one which is taken as an example of physisorbed CO_2. Fig. 8 clearly shows that the CO_2 derived peaks shift towards higher energies (lower binding energies) when going from the physisorbed long-top to the cross and long–long chemisorbed structures. However, for the three cases, the Na levels appear at the same energy. This is a clear indication that, in all cases, Na atoms have the same oxidation state. Therefore, the charge transfer can only be through the metal surface. Notice that the Na 2p-level shifts slightly upwards, but the reason is not a charge transfer, but a change in the Fermi level. This qualitative agreement permits to confirm that the species which is responsible for the experimental MIES and UPS spectra of CO_2 on Na-covered W(011) is in fact a negatively charged adsorbed CO_2 molecule. However, the quantitative disagreement in several respects reflects limitations on the model. On the one hand, the peaks on the DOS do only provide a qualitative guide to the ionization energies, final state effects are neglected. Here, one must advert that the computational model may not reproduce the experimental situation entirely. This is reflected in the fact that charge transfer is not enough. The Na coverage used is not small enough and a partial metallic phase develops. A smaller Na coverage will lead to a more ionic Na^+ adsorbed species,[37,39] and hence there will be a supply of extra electrons for the charge transfer, but, also, it would imply less positive charge to stabilize the charged carbon dioxide atoms and also a less favorable direct interaction of the CO_2 molecules with the Na adatoms. Nevertheless, the number of possible structures of adsorbed CO_2 studied in the present work is far from covering all possibilities. In any case, despite the energy level differences being significantly larger than in the physisorbed case, either CO_2 on the clean W(011) surface or on the long-top configuration for the Na covered W(011), the present results provide evidence that the Na-induced species CO_2 (chem), observed in the MIES and UPS spectra, is due to the activation of CO_2 which occurs through a partial charge transfer from the substrate to the molecule and results in a chemisorbed species.

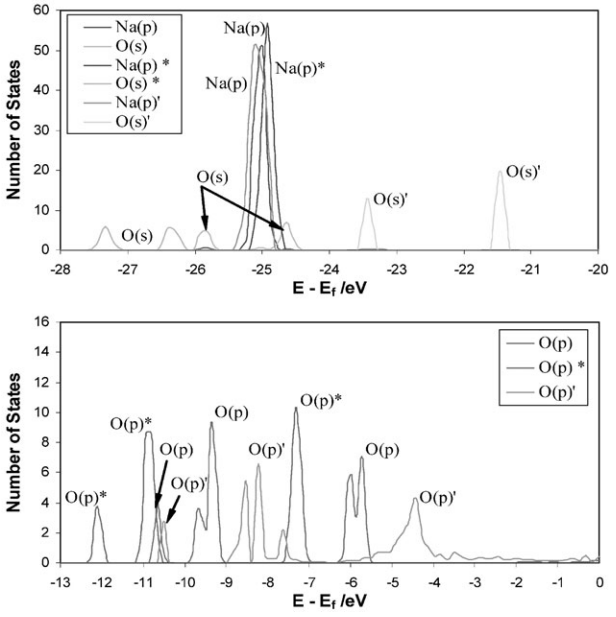

Fig. 8 LDOS of the CO_2 levels (contribution of the oxygen orbitals) and Na levels—cross, long-top (* projected densities of states) and long –long conformations ('projected densities of states).

The present theoretical and computational models explain details seen in the spectral changes occurring during the Na interaction with the CO_2 layer deposited at 80 K (Figs. 2 and 3): According to theory, Fig. 2 starts with a layer of physisorbed CO_2 (structure CO_2(phys)) whereby the C-atom has a distance of 3.4 Å from the tungsten surface. Na exposure leads to transfer of Na(3s) to the W conduction band (as manifested by the observed work function decrease) and to the adsorption of Na^+ species between the CO_2 layer and the substrate. The resulting structures are of the type "long top", characterized by a characteristic shift of the CO_2 induced features toward larger binding energies; at any rate, the initial phase of Na adsorption leads to a physisorbed species. Theory correctly predicts the shift of the spectral pattern towards larger binding energies as a consequence of the Na–CO_2 interaction. More Na supply is required to allow for configurations suited for the formation of CO_2(chem), *i.e.* of CO_2^- species, which becomes evident around 0.5 MLE Na coverage, and leads to a peak pattern compatible with the long–long structure. Theory correctly

predicts that peak ($1a_2$;$4b_2$) occurs at low binding energies, similar to that of $1\pi_g$ in CO_2(phys). Interestingly, there is no indication that the cross structure is formed during the interaction of Na with the CO_2 layer.

VI. Conclusions

The activation of CO_2 by interaction with Na atoms on W(011) has been studied by combining MIES, UPS (HeII) and first principles calculations. CO_2 physisorbs on pure W(011) in the range 80 to about 120 K; the distance between the three CO_2 spectral features is as in the gas phase ($E_B = 8.4$; 12.1; 14.1 eV). However, CO_2, offered to a Na monolayer on W(011), is converted into a chemisorbed species whereby, according to the first principles results, an initial transfer of 3sNa takes place to the W substrate, followed by "back donation" of charge from the substrate to the CO_2. As compared to physisorbed CO_2, the spectral pattern is different ($E_B = 6.3$; 10.7; 13.9 eV), and shows a global shift with respect to CO_2. The first principle calculations identify the chemisorbed species as distorted CO_2^- with an (O–C–O) bonding angle of 123°; these CO_2^- species are embedded into the Na adlayer. Chemisorption continues until all available Na species are converted to Na^+ species. Additional CO_2 offered to the system becomes physisorbed on top of the chemisorbed species.

When a CO_2 monolayer, physisorbed at 80 K, is exposed to Na, the interaction leads initially to a decrease of the surface work function and to a rigid, global shift of all CO_2 induced features towards larger binding energies by about 2 eV. First principles calculations show that, initially, transfer of the Na(3s) electron takes place to the substrate; but the spectral pattern remains essentially the same as for physisorption. Only beyond a minimum Na coverage of about 0.5 monolayers chemisorbed species can be detected. First principles calculations show that "back donation" of charge to CO_2 takes place whereby the physisorbed CO_2 species become converted to the distorted CO_2^- species also seen for adsorption on a Na film.

Acknowledgements

This research has been supported by the Spanish Ministerio de Educación y Ciencia (MEC) through grant BQU2002-04029-CO2-01 and, in part, by the Catalan Government through grants 2001SGR-00043 and Distinció de la Generalitat de Catalunya per a la Promoció de la Recerca Universitària (F.I.). F.V is grateful to MEC for a predoctoral grant. Computer time was provided by the Centre de Supercomputació de Catalunya, CESCA, Centre Europeu de Parallelisme de Barcelona, CEPBA, and CEBPA-IBM-Research Institute, CIRI, through generous grants from Universitat de Barcelona, Fundació Catalana per a la Recerca and CIRI.

References

1 F. Solymosi, *J. Mol. Catal.*, 1991, **65**, 337.
2 H. J. Freund and M. W. Roberts, *Surf. Sci. Rep.*, 1996, **25**, 225.
3 J. M. Ricart, M. P. Habas, A. Clotet, D. Curulla and F. Illas, *Surf. Sci.*, 2000, **460**, 170.
4 P. J. Godowski, J. Onsgaard, S. V. Hoffman and J. Nerlov, *Acta Phys. Pol., A*, 1999, **95**, 423.
5 J. Onsgaard, P. J. Godowski, J. Nerlov, S. Quist and S. V. Hoffmann, *Surf. Sci.*, 1998, **398**, 318.
6 J. Krause, D. Borgmann and G. Wedler, *Surf. Sci.*, 1996, **347**, 1.
7 J. Onsgaard, J. Storm, S. V. Christensen, J. Nerlov, P. J. Godowski, P. Morgen and D. Batchelor, *Surf. Sci.*, 1995, **336**, 101.
8 E. V. Thomsen, B. Jorgensen and J. Onsgaard, *Surf. Sci.*, 1994, **34**, 85.
9 J. A. Rodríguez, W. D. Clendening and C. T. Campbell, *J. Phys. Chem.*, 1989, **93**, 5238.
10 R. Hasender, D. Borgmann and G. Wedler, *Z. Phys. Chem.*, 1997, **198**, 157.
11 Th. Seyller, D. Borgmann and G. Wedler, *Surf. Sci.*, 1998, **400**, 63.
12 J. Nerlov, S. V. Christensen, S. Weichel, E. H. Pedersen and P. J. Moller, *Surf. Sci.*, 1997, **371**, 321.
13 H. Onishi and Y. Iwasawa, *Jpn. Catal. Lett.*, 1996, **38**, 89.
14 H. Onishi, T. Aruga, C. Egawa and Y. Iwasawa, *J. Chem. Soc., Faraday Trans. 1*, 1989, **85**, 2597.
15 J. M. Campbell, S. Reiff and J. H. Block, *Langmuir*, 1994, **10**, 3615.
16 P. Stracke, S. Krischok and V. Kempter, *Surf. Sci.*, 2001, **473**, 86.
17 S. Krischok, O. Höfft, J. Günster, J. Stultz, D. W. Goodman and V. Kempter, *Surf. Sci.*, 2001, **495**, 211.
18 Y. Harada, S. Masuda and H. Osaki, *Chem. Rev.*, 1997, **97**, 1897.
19 H. Morgner, *Adv. At. Mol., Opt. Phys.*, 2000, **42**, 387.
20 W. C. Price, in *Electron Spectroscopy: Theory, Techniques and Applications*, ed. C. R. Brundle and A. D. Baker, Academic Press, New York, 1977, vol. 1, p. 151.
21 M. Brause, S. Skordas and V. Kempter, *Surf. Sci.*, 2000, **445**, 224.
22 J. Perdew, J. A. Chevary, S. H. Vosko, K. A. Jackson, M. R. Pederson, D. J. Singh and C. Fiolhais, *Phys. Rev. B*, 1992, **46**, 6671.
23 P. E. Blöchl, *Phys. Rev. B*, 1994, **50**, 17953.
24 G. Kresse and D. Joubert, *Phys. Rev. B*, 1999, **59**, 1758.
25 G. Kresse and J. Hafner, *Phys. Rev. B*, 1993, **47**, 558.
26 G. Kresse and J. Furthmüller, *Comput. Mater. Sci.*, 1996, **6**, 15.
27 G. Kresse and J. Furthmüller, *Phys. Rev. B*, 1996, **54**, 11169.
28 W. Kohn, Y. Meir and D. E. Makarov, *Phys. Rev. Lett.*, 1998, **80**, 4153.
29 T. V. Mourik and R. J. Gdanitz, *J. Chem. Phys.*, 2002, **116**, 9620.
30 D. Ochs, M. Brause, W. Maus-Friedrichs and V. Kempter, *J. Electron Spectrosc. Relat. Phenom.*, 1998, **88–91**, 757.
31 D. Ochs, M. Brause, B. Braun, W. Maus-Friedrichs and V. Kempter, *Surf. Sci.*, 1998, **397**, 101.
32 W. Maus-Friedrichs, A. Gunhold, M. Frerichs and V. Kempter, *Surf. Sci.*, 2001, **488**, 339.
33 M. Frerichs, Diploma Thesis, TU Clausthal, 2002, unpublished.
34 S. Krischok, O. Höfft, J. Günster, R. Souda and V. Kempter, *Nucl. Instrum. Methods Phys. Res., Sect. B*, 2003, **124**, 203.
35 S. Krischok, O. Höfft and V. Kempter, *Surf. Sci.*, 2003, **370**, 532.
36 S. Krischok, O. Höfft and V. Kempter, *Surf. Sci.*, 2002, **69**, 507.
37 G. Pacchioni and P. S. Bagus, *Surf. Sci.*, 1992, **269/270**, 669–676.
38 B. J. Hopkins and K. R. Pender, *J. Appl. Phys.*, 1966, **17**, 281.
39 P. S. Bagus and G. Pacchioni, *Phys. Rev. Lett.*, 1993, **71**, 206.